Solid State Communications, Vol. 86, No. 8, pp. 497–502, 1993.
Printed in Great Britain.

0038–1098/93 $6.00 + .00
Pergamon Press Ltd

THE EFFECT OF PRESSURE ON THE ANTIFERROMAGNETIC AND SUPERCONDUCTING STATES OF HEAVY-FERMION UPd_2Al_3

K. Bakker, A. de Visser, L.T. Tai, A.A. Menovsky and J.J.M. Franse

Van der Waals — Zeeman Laboratorium, Universiteit van Amsterdam, Valckenierstraat 65, 1018 XE Amsterdam, The Netherlands

(*Received* 13 *January* 1993 *by P. Burlet*)

The effect of a hydrostatic pressure ($p \leq 3.5$ bar) on the antiferromagnetic ($T_N = 14.2$ K) and superconducting transition ($T_c = 1.9$ K) temperature of single-crystalline UPd_2Al_3 has been determined by means of resistivity measurements. The pressure effects are extremely small when compared to other heavy-fermion systems: $dT_N/dp = 0 \pm 3$ mK kbar^{-1} and $dT_c/dp = -2.0 \pm 0.7$ mK kbar^{-1}. The effect of a hydrostatic pressure ($p \leq 5$ kbar) on the antiferromagnetic phase boundary has been studied by means of high-field magnetization measurements ($B \leq 28$ T). It is found that the antiferromagnetic phase boundary, which is located at $B_c = 18$ T for a field in the hexagonal plane at $T = 5$ K, shifts to higher field values with pressure at a rate of 0.13 ± 0.01 T kbar^{-1}.

1. INTRODUCTION

THE OCCURRENCE of superconductivity in a select class of strongly correlated electron systems ($CeCu_2Si_2$, UBe_{13}, UPt_3 and URu_2Si_2) receives much attention because of the non-standard BCS nature of the superconducting condensate (for a review see e.g. [1–3]). In particular, the presence of pronounced antiferromagnetic spin-fluctuation phenomena, which co-build the heavy quasi-particles, has led to theoretical predictions that an unconventional Cooper state ($L \neq 0$), mediated by an antiferromagnetic electron–electron coupling mechanism, is realized in these systems. Besides, in most of the heavy-fermion superconductors a small-moment antiferromagnetically ordered state coexists with the superconducting state (except in the case of UBe_{13}), which raises the question of the interplay of antiferromagnetism and superconductivity. However, this issue is not easily addressed experimentally, not in the least because of the peculiar nature of the antiferromagnetic moment. The relevant experiments performed so far have primarily been successful in correlating the pressure dependences of the superconducting (T_c) and antiferromagnetic (T_N) transition temperatures.

Recently, the select class of antiferromagnetic heavy-electron superconductors was extended with UNi_2Al_3 ($T_N = 4.6$ K, $T_c = 1$ K) [4] and UPd_2Al_3 ($T_N = 14$ K, $T_c = 2$ K) [5], offering new possibilities to investigate the interplay of antiferromagnetism and superconductivity. Both compounds crystallize in the hexagonal $PrNi_2Al_3$ structure. Hitherto, single-crystalline samples have only been prepared for the Pd 1 : 2 : 3 compound and therefore UPd_2Al_3 has been characterized rather well experimentally [5–8]. The superconducting and antiferromagnetic phase diagrams show a number of interesting features [8]. As far as the superconductivity is concerned much attention is directed towards the possibility that a Fulde–Ferrell state is realized [9]. As to the antiferromagnetic properties, the fairly large ordered moment of $0.85 \pm 0.03\,\mu_B$ on the U-atom, detected by neutron diffraction [10], is conspicuous as it contrasts with the small ordered moments that have been reported for the other U-based heavy-fermion superconductors [3]. The magnetic properties are strongly anisotropic with the hexagonal plane as the easy plane for magnetization [6–8]. For $B = 0$, the ordering consists of ferromagnetic sheets parallel to the basal plane which are coupled antiferromagnetically along the hexagonal axis (c-axis), i.e. a doubling of the nuclear unit cell with an ordering vector $\mathbf{k} = [0, 0, 0.5]$. The antiferromagnetic phase diagram in the B–T plane consists of three phases with critical fields of 0.6 T, 4.2 T and 18 T (for $T \rightarrow 0$ and fields directed in the basal plane) [7, 8]. The magnetic structures of the field-induced phases are not yet resolved. Recently,

μSR experiments at temperatures as low as 50 mK indicate that antiferromagnetism and superconductivity coexist [11].

In this paper we report on the variation of T_c and T_N with hydrostatic pressure as determined by electrical resistivity measurements. Furthermore, we report on high-pressure high-field magnetization measurements which enabled us to study the pressure dependence of the antiferromagnetic phase boundary, which is located at $B_c = 18$ T at ambient pressure (for $T \to 0$).

2. EXPERIMENTAL

A single-crystalline batch of UPd_2Al_3 was prepared in a titanium gettered argon atmosphere using a modified tri-arc Czochralski technique. After an annealing procedure (7 days at 900°C) various samples were cut from the single-crystalline batch by means of spark erosion. For the high-pressure resistivity and high-pressure magnetization experiments a bar-shaped specimen was prepared (with dimensions $1 \times 1 \times 3.5\,mm^3$), with the long direction along the a-axis. Resistivity experiments performed for a current along the a-axis yield a residual resistance value $\rho_0 = 6.2\,\mu\Omega$ cm. The residual resistance ratio, $R(300\,K)/R(0\,K)$, equals 28. The onset for superconductivity occurs at $T_c^{onset} = 1.88$ K. The width of the superconducting transition is rather broad (0.2 K), which is ascribed to small variations in the aluminium concentration. Recently, single-crystalline material prepared with excess aluminium (nominal composition $UPd_2Al_{3.03}$) [12], was found to exhibit a much sharper resistive superconducting transition. Possibly, excess starting material compensates for the evaporation of aluminium during the crystal growth procedure.

For the resistivity experiments under pressure the sample was mounted on a support with current and potential leads attached to it by means of soldering. The support and sample were placed in a pressure vessel (cylindrical shape, outer diameter 25 mm, inner diameter 6 mm), constructed of a copper–beryllium alloy. The high-pressure low-temperature electrical feedthrough was realized by embedding the wires in epoxy and gluing them on a conically machined plug that served as pressure sealing. Helium was used as pressure transmitting medium. The pressure cell was connected to the pressure generating unit via a flexible stainless-steel capillary tube. As in the pressure-temperature range where we performed our experiments the helium gas solidifies, special care was taken in order to preserve hydrostaticity. This was realized by cooling the pressure vessel slowly, while maintaining a temperature gradient, as to start solidification at the bottom of the cell. The pressure was monitored by strain gauges that were glued on the pressure vessel.

The magnetization experiments under pressure were performed in the High Magnetic Field Facility of the University of Amsterdam [13]. The sample was mounted in a cylindrical pressure vessel with strongly reduced dimensions (outer diameter 5 mm, inner diameter 1.7 mm). The vessel was machined of a copper–beryllium alloy. Again helium was used as the pressure transmitting medium. The pressure cell with sample was placed in a compensated pick-up coil system. The magnetization was measured by integrating the induced voltage. In the high-field installation pulsed magnetic fields can be generated up to 40 T, with a total pulse time of about 1 s. The energy is taken directly from the mains. Different pulse shapes can be chosen as the field can be regulated by a thyristor rectifier that is coupled to the mains. An experimental difficulty when using metallic pressure vessels in pulsed magnetic fields at low temperatures is the generation of heat due to the dissipation of eddy currents. As the pressure-transmitting solid helium is a good thermal conductor, the temperature of the sample might change. In order to keep the temperature raised of the sample within acceptable limits, a low field sweep rate of $30\,T\,s^{-1}$ was chosen. Furthermore, the pressure vessel and pick-up coil were immersed directly in liquid helium (at atmospheric pressure). The effective temperature of the sample during the magnetic field pulse amounts to 5.0 ± 0.3 K. The data at various pressures have been taken for increasing fields, using identical field profiles. The as-measured signal was corrected for the remaining unbalance of the pick-up coil system and the signal from the empty pressure vessel. In the high-field range the magnetization of the sample exceeds that of the pressure cell by a factor 5.

3. RESULTS AND ANALYSIS

The electrical resistivity of UPd_2Al_3 for a current along the a-axis at ambient pressure for $T < 300$ K is shown in Fig. 1. The increase in $\rho(T)$ with decreasing temperature is ascribed to a mixture of Kondo and crystalline electric field effects, yielding a broad maximum centred at 80 K. At low temperatures, in the coherent state, a pronounced kink is observed, which signals the antiferromagnetic transition at $T_N = 14.2$ K. Superconductivity is found below 1.88 K. These zero-pressure data are in good agreement with previous reports [5, 14]. Under hydrostatic pressures up to 3.5 kbar only minute

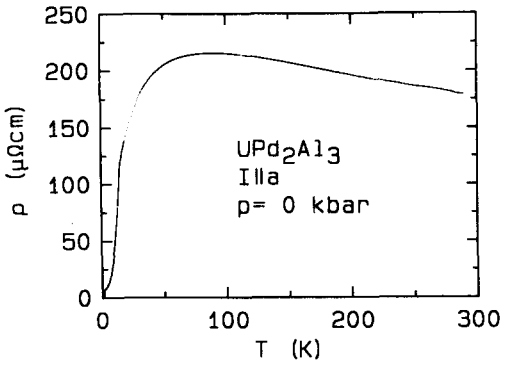

Fig. 1. Temperature dependence of the electrical resistivity of single-crystalline UPd_2Al_3 ($I \parallel a$) at $p = 0$ kbar.

changes of the resistivity curve are observed. In Figs. 2 and 3 we show $\rho(T)$ at ambient pressure and $p = 3.5$ kbar, in the vicinity of T_N and T_c, respectively. The effect of pressure on T_N is negligibly small: $dT_N/dp = 0 \pm 3$ mK kbar^{-1}. The effect of pressure on T_c is negative, but very small: $dT_c/dp = -2.0 \pm 0.7$ mK kbar^{-1}. The width of the superconducting transition is rather large (0.2 K) and does not change with pressure, indicating that the entire sample reacts in the same way under pressure. An additional curve at $p = 2.0$ kbar (not shown) was found to be intermediate between the curves at 0 and 3.5 kbar.

The sudden drop of $\rho(T)$ at T_N for UPd_2Al_3 contrasts with the increase in resistivity just below T_N as observed for the heavy-fermion antiferromagnets URu_2Si_2 ($T_N = 17.5$ K) [15] and $U(Pt_{0.95}Pd_{0.05})_3$ ($T_N = 5.8$ K) [16]. In the latter compounds the antiferromagnetic transition of the spin-density wave type is accompanied by the formation of a gap over a part of the Fermi surface. In the case of URu_2Si_2, the normal-state electrical resistivity below T_N could satisfactorily be analyzed using the expression for an antiferromagnet with an energy

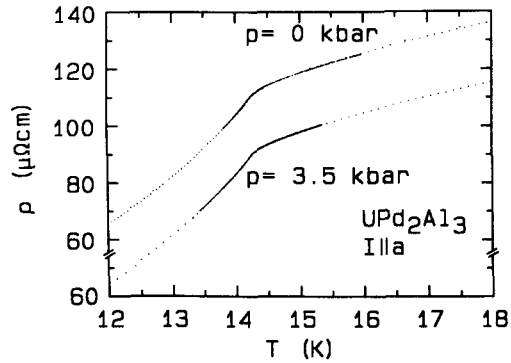

Fig. 2. Electrical resistivity of single-crystalline UPd_2Al_3 ($I \parallel a$) around T_N for $p = 0$ and $p = 3.5$ kbar as indicated.

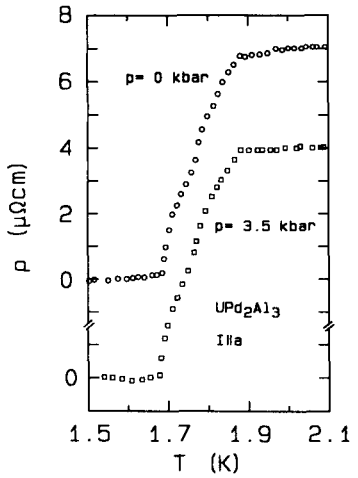

Fig. 3. Electrical resistivity of single-crystalline UPd_2Al_3 ($I \parallel a$) around T_c for $p = 0$ (○) and $p = 3.5$ kbar (□).

gap, Δ (of the order of 80 K), and a T^2-term due to the Fermi-liquid behaviour [15]:

$$\rho = \rho_0 + BT[1 + 2T/\Delta]\exp(-\Delta/T) + AT^2. \quad (1)$$

Figure 4 shows that the $\rho(T)$-data ($I \parallel a$) of UPd_2Al_3 are described reasonably well using equation (1). The optimum fit parameters are: $\rho_0 = 6.2\,\mu\Omega$ cm, $B = 30\,\mu\Omega$ cm K^{-1}, $\Delta = 39$ K and $A = 0.24\,\mu\Omega$ cm K^{-2}. Recently, the resistivity of polycrystalline UPd_2Al_3 was analyzed in a similar way by Dalichaouch *et al.* [14], yielding $\Delta = 40$ K. Hence, the resistivity data suggest that also in UPd_2Al_3 a gap is formed at T_N. On the other hand, close to T_N, small deviations from equation (1) appear, while also the typical increase in $\rho(T)$ below T_N due to the decrease of carriers is absent. A careful analysis of the electronic specific heat, including an

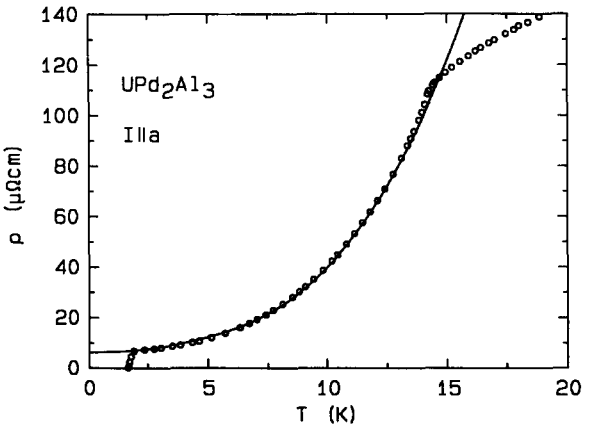

Fig. 4. Low-temperature electrical resistivity of single-crystalline UPd_2Al_3 ($I \parallel a$) at zero pressure. The solid line represents the optimum fit to equation (1) (see text).

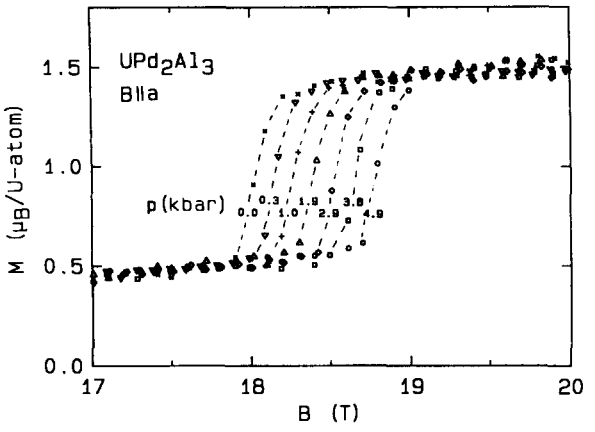

Fig. 5. Magnetization of single-crystalline UPd_2Al_3 ($B \parallel a$) for pressures up to 4.9 kbar as indicated ($T = 5$ K).

exponential term, might further elucidate this point. A fit of the $\rho(T)$ data under pressure to equation (1) yields identical parameters ρ_0, A, B and Δ within the accuracy of the analysis.

Next, we present the results of the high-pressure high-field magnetization experiments. At ambient pressure at $T = 4.2$ K the magnetization of UPd_2Al_3 for a field in the hexagonal plane shows a sharp jump at $B_c = 18.0$ T [7]. As the size of the jump ($\Delta M = 0.92\,\mu_B$/U-atom) is almost equal to the size of the ordered moment ($0.85\,\mu_B$/U-atom), the transition at B_c most likely reflects the antiferromagnetic phase boundary. Under pressure B_c shifts to higher fields as is shown in Figs. 5 and 6. In the pressure range 1 kbar $< p <$ 4.9 kbar, B_c increases linearly with pressure at a rate $dB_c/dp = 0.13 \pm 0.01$ T kbar^{-1}. At smaller pressures the variation of B_c is non-linear. The variation of the magnetization with pressure, $M(p)$, above and below B_c, cannot

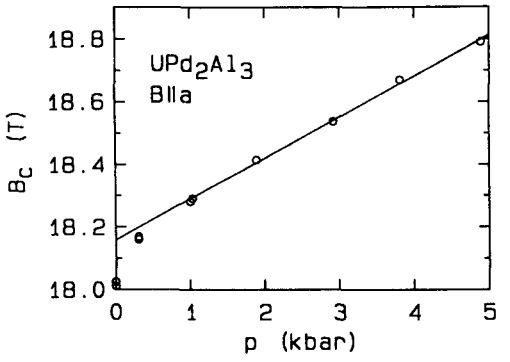

Fig. 6. Pressure variation of B_c for single-crystalline UPd_2Al_3 ($B \parallel a$) at $T = 5.0 \pm 0.3$ K. The solid line indicates the linear regime for pressures $p >$ 1 kbar: $dB_c/dp = 0.13$ T kbar^{-1}.

be determined from the present experiments, as it falls within the experimental uncertainty ($0.1\,\mu_B$/U-atom). The overall effect on the $M(B)$ curve is very small for the applied pressures. Also, the pressure variation of the size of the jump at B_c is negligibly small: $d\Delta M/dp = 0 \pm 0.4 \times 10^{-2}$ (μ_B/U-atom) kbar^{-1}.

4. DISCUSSION

In general, the low-temperature properties of heavy-fermion systems are extremely sensitive to pressure, because of the strong hybridization of the f-orbitals of Ce or U with the p or d-orbitals of the ligand atoms. Consequently, large Grüneisen parameters are found for the volume variation of the characteristic temperature, T^*, below which the heavy quasiparticle bands are formed: $\Gamma = -\partial \ln T^*/\partial \ln V \simeq 100$ [17]. As the heavy quasiparticles participate in the formation of the superconducting and antiferromagnetic states, also T_c and T_N depend strongly on pressure, e.g. for UPt_3 $\Gamma_{sc} = -\partial \ln T_c/\partial \ln V = -52$ [18], for $U(Pt_{0.95}Pd_{0.05})_3$ $\Gamma_{af} = -\partial \ln T_N/\partial \ln V = -110$ [19] and for URu_2Si_2 $\Gamma_{sc} = -62$ and $\Gamma_{af} = 16$ [20] (note that in the case of URu_2Si_2 the Grüneisen parameters are calculated with an estimated compressibility $\kappa = 0.73$ Mbar^{-1}). These large values clearly contrast with the small values observed for UPd_2Al_3: $\Gamma_{sc} = -1 \pm 0.4$ and $\Gamma_{af} = 0 \pm 0.2$ (here we used an estimated compressibility $\kappa = 1$ Mbar^{-1}). As the pressure dependence of T_c is concerned, the small value of Γ_{sc} is in agreement with the near absence of a discontinuity at T_c in the coefficients of thermal expansion, measured for a single-crystalline sample along ($\alpha_\parallel$) and perpendicular to ($\alpha_\perp$) the hexagonal axis [6] (conform the Ehrenfest relation). Note that Γ_{af} has not been determined reliably yet via thermal expansion, as data have only been obtained for a polycrystalline sample with preferentially oriented crystallites [6].

Apparently, superconductivity and antiferromagnetism in UPd_2Al_3 are correlated in the sense that both are rather insensitive to pressure. It is interesting to note that the very weak pressure dependence of T_c (and probably also of T_N) does not result from a near cancellation of the uniaxial pressure effects, as $\alpha_\parallel$ and $\alpha_\perp$ show no large discontinuities at T_c. Hence, both uniaxial and hydrostatic pressure effects are small. This strongly suggests that the hybridization effects in UPd_2Al_3 are less important than in other heavy-fermion compounds and, consequently, a more localized

character of the *f*-electrons is inferred. This claim is supported by the relatively large size of the ordered moment.

Although T_N is almost pressure independent, the low-temperature antiferromagnetic phase boundary shifts upwards at a rate $dB_c/dp = 0.13\,T\,kbar^{-1}$, indicating a stronger antiferromagnetic coupling under pressure. The actual magnetization process, with the hexagonal plane as easy plane for magnetization, is far from being unravelled. The zero-pressure high-field magnetization [7] and magnetoresistance [21] experiments yield one sharp transition at $B_c = 18\,T$, which reflects the antiferromagnetic phase boundary, and the absence of a marked basal-plane anisotropy. However, in a further detailed investigation a small basal-plane anisotropy was detected [22]. This possibly suggests that the transition at B_c is of the spin-flip type. Furthermore, recent magnetization, magnetrostriction and magnetoresistance experiments have revealed the presence of two additional phase lines (with critical fields of 0.6 T and 4.2 T for $T \to 0$) indicating that the paramagnetic state is reached via two field-induced magnetic phases [8]. Neutron-diffraction experiments in a magnetic field would be most welcome to elucidate the magnetic structures of the various phases.

In conclusion, we have studied the pressure dependence of the superconducting (T_c) and antiferromagnetic (T_N and B_c) phase boundary of UPd_2Al_3 via resistivity and magnetization experiments. The deduced pressure variations are much smaller than observed for other heavy-fermion compounds, suggesting a dominant local character of the *f*-electrons.

Acknowledgements — The research of one of us (AdV) was made possible by a fellowship of the Royal Netherlands Academy of Arts and Sciences. S.A.M. Mentink is gratefully acknowledged for a first characterization of the sample. The authors thank R. Scheltema for skilful assistance during the experiments.

REFERENCES

1. H.R. Ott, in: *Progress in Low Temp. Physics Vol. XI* (Edited by D.F. Brewer), p. 215. North-Holland, Amsterdam (1987).
2. N. Grewe and F. Steglich, in: *Handbook on the Physics and Chemistry of Rare Earths Vol.* 14 (Edited by K.A. Gschneidner, Jr. & L. Eyring), p. 343. North-Holland, Amsterdam (1991).
3. A. de Visser & J.J.M. Franse, *J. Magn. Magn. Mat.* **100,** 204 (1991).
4. C. Geibel, S. Thies, D. Kaczorowski, A. Mehner, A. Grauel, B. Seidel, U. Ahlheim, R. Helfrich, K. Petersen, C.D. Bredl & F. Steglich, *Z. Phys.* **B83,** 305 (1991).
5. C. Geibel, C. Schank, S. Thies, H. Kitazawa, C.D. Bredl, A. Böhm, M. Rau, A. Grauel, R. Caspary, R. Helfrich, U. Ahlheim, G. Weber & F. Steglich, *Z. Phys.* **B84,** 1 (1991).
6. C. Geibel, U. Ahlheim, C.D. Bredl, J. Diehl, A. Grauel, R. Helfrich, H. Kitazawa, R. Köhler, R. Modler, M. Lang, C. Schank, S. Thies, F. Steglich, N. Sato & T. Komatsubara, *Physica* **C185–189,** 2651 (1991).
7. A. de Visser, H. Nakotte, L.T. Tai, A.A. Menovsky, S.A.M. Mentink, G.J. Niewenhuys & J.A. Mydosh, *Physica* **B179,** 84 (1992).
8. A. Grauel, A. Böhm, H. Fischer, C. Geibel, R. Köhler, R. Modler, C. Schank, F. Steglich, G. Weber, T. Komatsubara & N. Sato. *Phys. Rev.* **B46,** 5818 (1992).
9. F. Steglich *et al.*, in: *Proceedings of the Hiroshima Workshop on Transport and Thermal Properties of f-Electron Systems,* Hiroshima, August 30–September 2, (1992) (to be published).
10. A. Krimmel, P. Fischer, B. Roessli, H. Maletta, C. Geibel, C. Schank, A. Grauel, A. Loidl & F. Steglich, *Z. Phys.* **B86,** 161 (1992).
11. A. Amato, R. Feyerherm, F.N. Gygax, A. Schenck, M. Weber, R. Caspary, P. Hellmann, C. Schank, C. Geibel, F. Steglich, D.E. MacLaughlin, E.A. Knetsch & R.H. Heffner, *Europhys. Lett.* **19,** 127 (1992).
12. T. Sakon, K. Imamura, N. Takeda, N. Sato & T. Komatsubara, in: *Proc. Int. Conf. on Strongly Correlated Electron Systems*, Sendai, 7–11 September (1992) (to be published).
13. R. Gersdorf, F.R. de Boer, J.C. Wolfrat, F.A. Muller & L.W. Roeland, in: *High Field Magnetism* (Edited by M. Date), p. 277. North-Holland, Amsterdam (1983).
14. Y. Dalichaouch, M.C. de Andrade & M.B. Maple, *Phys. Rev.* **B46,** 8671 (1992).
15. T.T.M. Palstra, A.A. Menovsky & J.A. Mydosh, *Phys. Rev.* **B33,** 6527 (1986).
16. R. Verhoef, A. de Visser, A. Menovsky, A.J. Riemersma & J.J.M. Franse, *Physica* **B142,** 11 (1986).
17. A de Visser, J.J.M. Franse & J. Flouquet, *Physica* **B161,** 324 (1989).
18. J.O. Willis, J.D. Thompson, Z. Fisk, A. de Visser, J.J.M. Franse & A. Menovsky, *Phys. Rev.* **B31,** 1654 (1985).
19. J.J.M. Franse, K. Kadowaki, A. Menovsky, M. van Sprang & A. de Visser, *J. Appl. Phys.* **61,** 3380 (1987).

20. K. Bakker, A. de Visser, E. Brück, A.A. Menovsky & J.J.M. Franse, *J. Magn. Magn. Mat.* **108,** 63 (1992).
21. A. de Visser, K. Bakker, L.T. Tai, A.A. Menovsky, S.A.M. Mentink, G.J. Nieuwenhuys and J.A. Mydosh, in: *Proc. Int. Conf. on Strongly Correlated Electron Systems*, Sendai, 7–11 September (1992) (to be published).
22. A de Visser *et al.* (to be published).